J Oceanogr (2011) 67:197–208
DOI 10.1007/s10872-011-0018-3

ORIGINAL ARTICLE

Linkage between winter air temperature over the subtropical Western Pacific and the ice extent anomaly in the Sea of Okhotsk

Xiao-Yi Yang · Jianyu Hu · Jia Wang · Daoru Wang

Received: 22 November 2010 / Revised: 31 January 2011 / Accepted: 28 February 2011 / Published online: 23 March 2011

Abstract This study deals with the correlation between ice extent in the Sea of Okhotsk and the interannual variability of winter (December–February) air temperature over the subtropical Western Pacific from 1979 to 2008. The analysis indicates that the increase in sea ice extent coincides not only with cooling over the Sea of Okhotsk and the adjacent area, but also with significant warming over the subtropical Western Pacific that extends from the surface to the middle troposphere. This meridional dipole pattern of tropospheric temperature anomalies (cooling in the high latitudes and warming in the low latitudes) primarily results from dynamical processes driven by the large-scale atmospheric circulation change. A heat budget diagnosis reveals that when ice extent in the Sea of Okhotsk increases by one standard deviation, the tropospheric air temperature over the subtropical Western Pacific rises by about 0.25°C. It also suggests that the adiabatic heating and stationary eddy heat flux convergence may be the most important factors, which account for 30 and 15% of the warming, respectively. In addition, these two factors also coordinate to result in significant cooling over the Sea of Okhotsk and the adjacent regions.

X.-Y. Yang (✉) · J. Hu
State Key Laboratory of Marine Environmental Science, Xiamen University, Xiamen, Fujian, China
e-mail: xyyang@xmu.edu.cn

J. Wang
NOAA Great Lakes Environmental Research Laboratory, Ann Arbor, MI, USA

D. Wang
Hainan Marine Development and Design Institute, Haikou, Hainan, China

Keywords Western Pacific · Sea ice extent · The Sea of Okhotsk · Thermal feedback · Heat budget · Meridional temperature advection · Eddy heat flux

1 Introduction

The subtropical Western Pacific (WP) is famous both for its importance in the climate system and for the complexity of ocean–atmosphere interaction mechanisms. A large thermal contrast between the Far East Eurasia continent and the ocean drives the seasonal alternation of meridional wind—the so-called East Asian monsoon (Wu and Wang 2002; Wang et al. 2010a), which exerts a far-reaching effect on the global climate. Besides the east–west thermal contrast, this region is also characterized by a strong north–south thermal gradient. To the south is the warm pool, and to the north is the Sea of Okhotsk (OS) that is covered with the seasonal sea ice. The strong meridional thermal gradient favors the intensification of the East Asian jet stream, and is related to variations of the mid-latitude storm track (Wang et al. 2004).

A number of studies have investigated the interannual variability of wintertime climate in the East Asia–Western Pacific area. The most important players include: the El Niño–Southern Oscillation (Wang et al. 1999; Lau and Nath 2000; Wang et al. 2000), the Arctic Oscillation (Gong et al. 2001; Wang and Ikeda 2000), the Siberian High (Gong and Ho 2002; Wu and Wang 2002; Wang et al. 2010a) and the Aleutian Low (Rodionov et al. 2005). In addition to the inherent atmosphere–ocean mode, other internal forcing factors like snow cover and sea ice may play a role in modulating the winter climate variation. Clark and Serreze (2000) reported that the East Asian snow cover retreat is associated with the weakening of the East

Asian jet and the Aleutian Low, and the decrease in eddy activity in the mid-latitude storm track. By identifying two leading modes of the North Pacific sea ice variability, Liu et al. (2007) suggested that ice decrease in the OS and increase in the Bering Sea tend to induce an anomalous anticyclone and weakening of the East Asian jet stream and trough, whereas the simultaneous ice decrease in the whole North Pacific region coincides with the anomalous cyclone, the strengthening of the East Asian jet stream and trough, and the intensified East Asian Winter Monsoon (EAWM). Although these results based on the empirical orthogonal function (EOF) analysis are very useful for understanding the sea ice variability and its impact on the winter climate, the interpretation of the physical mechanism remains ambiguous. The reasons for this ambiguity can be speculated from two aspects: (1) the EOF analysis is a mathematical method, but not essentially inherent to physical modes (Ambaum et al. 2001); thus the dipole mode of sea ice (PC1) does not reflect the real negative correlation between the Bering Sea ice and the OS ice. According to our calculation, the correlation coefficient of the winter sea ice extent in the two seas is barely significant (−0.083 for the raw data, and −0.253 for the detrended data from 1979 to 2008). In this sense, the Bering Sea ice and the OS ice vary independently; and (2) the PC1 and PC2 modes are, respectively, characterized by the ice concentration increase and decrease in the Bering Sea, but that in the OS shows no notable change in the two modes. Hence Liu et al.'s results may largely indicate the strong correlation between large-scale atmospheric circulation anomalies and the ice anomaly in the Bering Sea, but not in the OS.

Previous studies have investigated the atmospheric forcing of the OS ice (e.g., Parkinson 1990; Fang and Wallace 1994; Sasaki et al. 2007). Honda et al. (1999) demonstrated that the OS ice, in turn, can feed back to the atmospheric circulation through a thermally generated stationary Rossby wave, and then induce the atmospheric responses downstream over the Bering Sea, Alaska, and North America. So far, these studies have all focused on the mid- to high-latitude atmospheric circulation change, as the general consensus is that the thermal effect of sea ice diminishes rapidly with distance (e.g., Raymo et al. 1990; Chiang and Bitz 2005), especially over the oceans (Parkinson et al. 2001). Less known is the correlation between the OS ice anomaly and the WP climate in the lower latitudes.

This study aims to explore the connection between the winter air temperature over the WP and the OS ice extent anomaly. The paper is organized as follows: Sect. 2 introduces the data and methods used in this study. Section 3 deals with the correlation between temperature change and the anomalous OS ice extent, which is followed by analyzing the related atmospheric circulation change in Sect. 4. In Sect. 5, a thermodynamic equation is used to diagnose the factors that are sensitive to the OS ice change and contribute to the remote response of temperature over the subtropical WP. Section 6 gives a summary and discussion.

2 Data and methods

Monthly mean sea ice concentration (SIC) and sea surface temperature (SST) data were obtained from the UK Hadley Centre Global Ice and SST (HadISST) dataset on a 1° latitude by 1° longitude grid from 1871 to the present. The SIC data are a merged dataset of several sources, including the Northern Hemisphere SIC charts (Walsh 1995), the National Ice Centre charts, and passive microwave retrievals (Rayner et al. 2003). Here we chose the SIC data for the period 1979–2008 when the satellite observations were available for assimilation (Armstrong et al. 2003).

Another dataset is the National Centers for Environmental Prediction–National Center for Atmospheric Research (NCEP/NCAR) reanalysis dataset, with a horizontal resolution of 2.5° latitude by 2.5° longitude, and a vertical resolution of 17 levels from 1,000 hPa up to 10 hPa (Kalney et al. 1996). This dataset includes air temperature, geopotential height, and zonal and meridional velocities. The surface air temperature and net sensible heat flux are also used. The monthly heat flux due to standing and transient eddies are computed with daily temperature and horizontal velocity fields and averaged for each month.

For each year from 1979 to 2008, the winter (December–February) mean is calculated, and the anomalies are obtained by subtracting the 30-year climatology from the individual winter seasons. We then estimate the 30-year linear trends for all the variables on each grid and subtract them from the data. The detrending procedure applied here filters out the long-term change in the interdecadal timescale, and keeps the results from being obscured by the global warming signals. To assess the atmospheric circulation change associated with the OS ice, the various physical variables were linearly regressed on the normalized OS ice extent index. The regression coefficients, in this sense, can be interpreted as the variations corresponding to the OS ice extent above one standard deviation. Here it is worth noting that using the linear regression method we still cannot decide the cause and effect of the relationship between the air temperature and the OS ice extent.

3 Temperature dipole pattern in accordance with the OS ice

Before investigating the temperature variability, we first review the seasonal cycle of OS ice cover and its

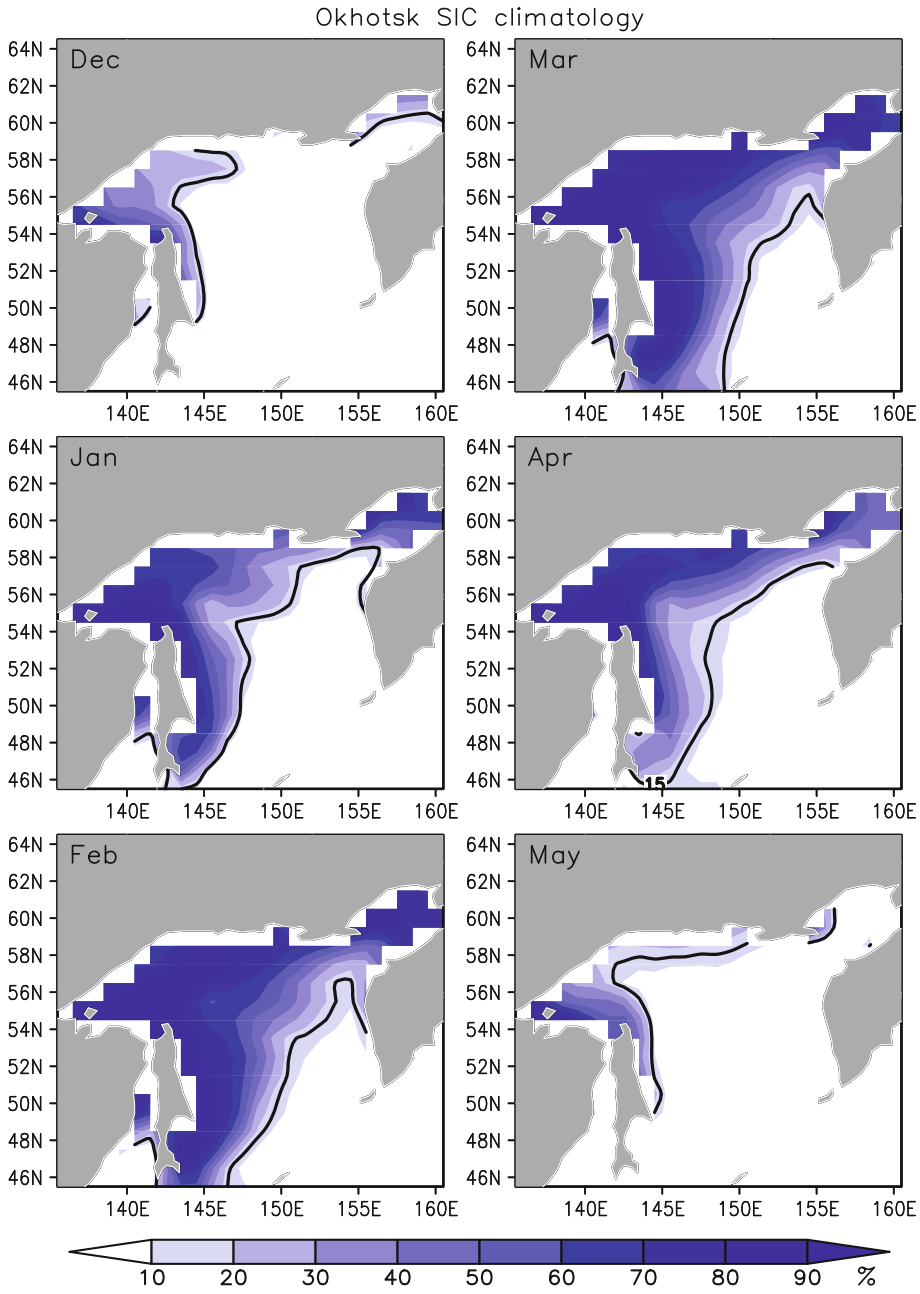

Fig. 1 December–May climatology of the Sea of Okhotsk ice concentration (SIC) for the period from 1979 to 2008 (unit %). The Sea of Okhotsk ice extent is defined as the total area of sea ice cover above 15% of SIC (*black bold lines*)

thermodynamic effect on the ocean–atmosphere interaction. As shown in the monthly climatology of SIC (Fig. 1), the ice starts to grow in late autumn/early winter along with the establishment of semipermanent active centers of Siberian High and Aleutian Low as well as the prevailing of the EAWM, and retreats in late spring. The seasonal cycle of sea ice cover mediates the net air–sea sensible heat flux to a large extent, with the maximal heat flux from the ocean to the atmosphere in December and thereafter slowly decreasing owing to the insulation effect of ice cover. The weak negative heat flux (from the atmosphere to the ocean) appears in late spring when the ice retreats (not shown). Thus the winter OS ice extent anomaly has the potential to impact the surface air temperature variability and local climate.

To represent the variability of OS ice cover, sea ice extent is defined as the total area represented by grid points that are more than 15% covered by sea ice (as indicated by bold lines in Fig. 1). The winter OS ice extent index (OSI) is constructed by using the normalized winter (December–February) mean sea ice extent for each year (Fig. 2). The winter SST and surface air temperature (SAT) anomalies in accordance with the OSI above +1 standard deviation are shown in Fig. 3a, b, respectively. When the OS ice extent

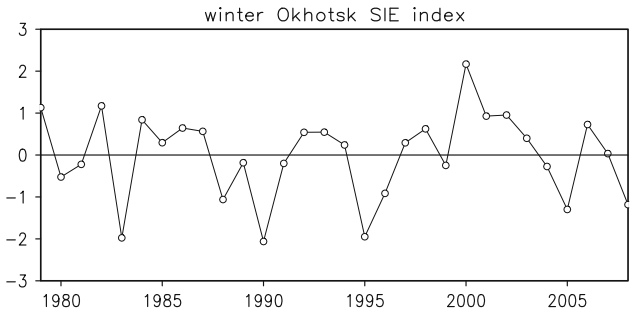

Fig. 2 Normalized winter (December–February) mean Okhotsk Sea ice extent index (OSI)

increases, both the SST and SAT decrease in the OS and the adjacent area, and the cold anomalies tend to be advected downstream to the Central and Eastern Pacific. At the same time, the warm anomalies can be found over the Bering Sea, Alaska, and the low latitudes of WP (southward of 40°N). The warming in the Bering Sea and Alaska has been reported as a remote response to the OS ice anomaly due to the stationary wave activity (Honda et al. 1999). But this meridional response in the low latitudes of WP, from the South China Sea up to the Sea of Japan, has not been investigated. We further take the 120–160°E mean air temperature to examine the tropospheric temperature anomalies (Fig. 3c). The meridional dipole pattern, with negative (positive) anomaly poleward (equatorward) of 40°N, extends from the surface to the middle troposphere. There is somewhat a reversal of signs in the upper troposphere, indicating the overall baroclinic structure of the sea ice-related response. It is worth noting that the maximal warming over the WP occurs at the lower troposphere (about 850 hPa), whereas the maximal cooling in the high latitudes is located near the surface. This implies that the lower tropospheric circulation change may play a key role in driving the WP air temperature change.

4 Atmospheric circulation patterns corresponding to the sea ice anomaly

It is well known that reduction (expansion) in sea ice cover coincides with the atmospheric warming (cooling) over that surface that expands to lower latitudes through horizontal advection and eddy transport (Royer et al. 1990; Budikova 2009). However, the linkage between the WP warming over the Kuroshio region and the OS ice expansion shown in Fig. 3 requires more in-depth analysis from both thermodynamic and dynamic viewpoints.

Figure 4 shows the climatology of surface net sensible heat flux and its regression coefficient pattern on the OSI. In winter, strong positive values of sensible heat flux (from the ocean to the atmosphere) appear in the WP, in compensating the large thermal contrast at the air–sea surface due to the warm Kuroshio and the cold EAWM (Fig. 4a). In accordance with increasing ice cover the sensible heat flux decreases greatly at the western OS, owing to the direct insulation effect of sea ice. On the other side, the large-scale SAT and SST anomalous dipole patterns (Fig. 3a, b) coincide with the significant increasing upward heat flux in the high latitude ice-free region and decreasing heat flux at the lower latitude (Fig. 4b).

The remarkable subtropical warming at the lower troposphere is more closely related to the atmospheric circulation change than to the surface thermal conditions. The increase of sea ice cover corresponds to the decrease of sea level pressure over the North Pacific region, hence the strengthening of the climatologic Aleutian Low (Fig. 5a). The deepened Aleutian Low, along with the Siberian High, drives anomalous strong EAWM that advects the cold, dry air from the Arctic to the OS. In the middle troposphere, a dipole pattern of geopotential height is associated with the sea ice cover extension, denoting the deepening (shallowing) of the East Asian trough poleward (equatorward) of 40°N (Fig. 5b). Along with the geopotential height anomalies are the cyclone (anticyclone) circulation in the high (low) latitudes (Fig. 5c), and intensification of the upper tropospheric jet stream (Fig. 5d).

5 Heat budget

Winter climate over the Western Pacific–East Asia is characterized by a deep East Asian trough, an Aleutian Low, and the prevailing of EAWM (Wu and Wang 2002; Wang et al. 2010a). These circulation systems are expected to impact the temperature variability via the stationary eddy heat flux and meridional temperature advection. We conducted the heat budget analysis by recognizing these important processes (Fig. 6). In climatology, the lower tropospheric cold advection and the strong poleward heat flux due to the stationary wave activity dominate the WP (Fig. 6a, c). During the winter, an increase of ice in the OS and the anomalous northerly (southerly) winds associated with the cyclonic (anticyclonic) circulation anomaly (Fig. 5c) lead to the cold (warm) advection anomaly poleward (equatorward) of 40°N (Fig. 6b). At the same time, the ice-related dipole pattern of geopotential height (Fig. 5b) tends to intensify (reduce) the stationary wave activity, resulting in more (less) poleward heat flux. This behavior leads to the heat flux divergence (convergence) anomalies, thus the cooling (warming) in the high (low) latitudes (Fig. 6d).

Although correlations between the OSI and various atmospheric circulation variables are significant, the

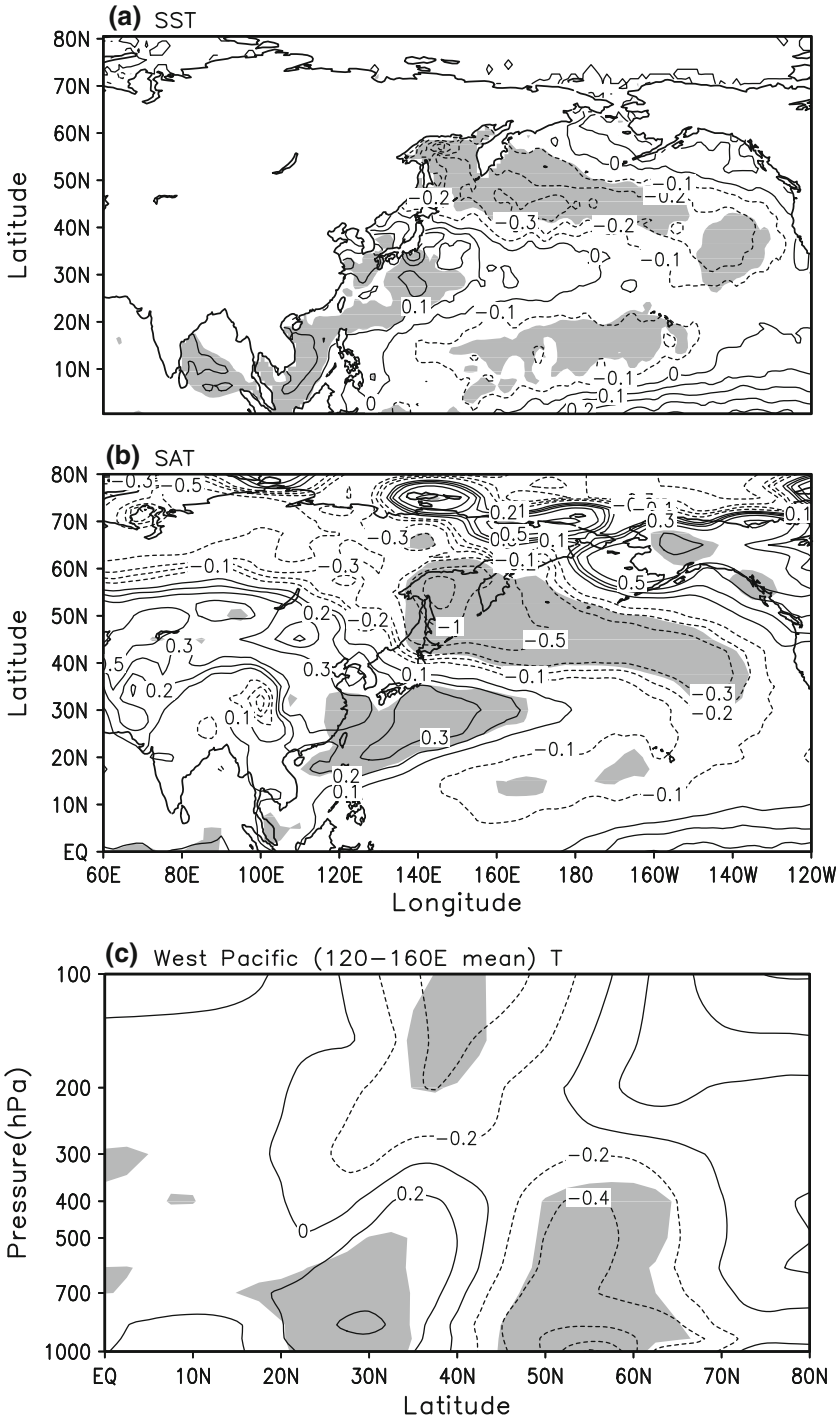

Fig. 3 **a** Regression coefficients of winter (December–February) mean sea surface temperature (SST) on the normalized OSI, representing the SST anomalies in accordance with the OSI above +1 standard deviation (unit °C). *Shaded areas* denote that the regression coefficients are significant at the 95% level. Same as **a**, but for **b** surface air temperature and **c** latitude–pressure section of tropospheric air temperature over the Western Pacific (120–160°E mean) region

regression coefficients are relatively small. For example, the net sensible heat flux anomalies (Fig. 4), 850 hPa temperature advection anomalies, and stationary eddy heat flux anomalies (Fig. 6) corresponding to OSI above one standard deviation are only less than 10% of their climatology. Is it possible that these small changes in the atmospheric circulation lead to the warming over the subtropical WP and which processes are dominant? We further resort to the heat budget analysis to study the major factors that are responsible for the anomalous dipole pattern in the WP (120–160°E mean). Here the thermodynamic equation in pressure coordinates is written in the form of:

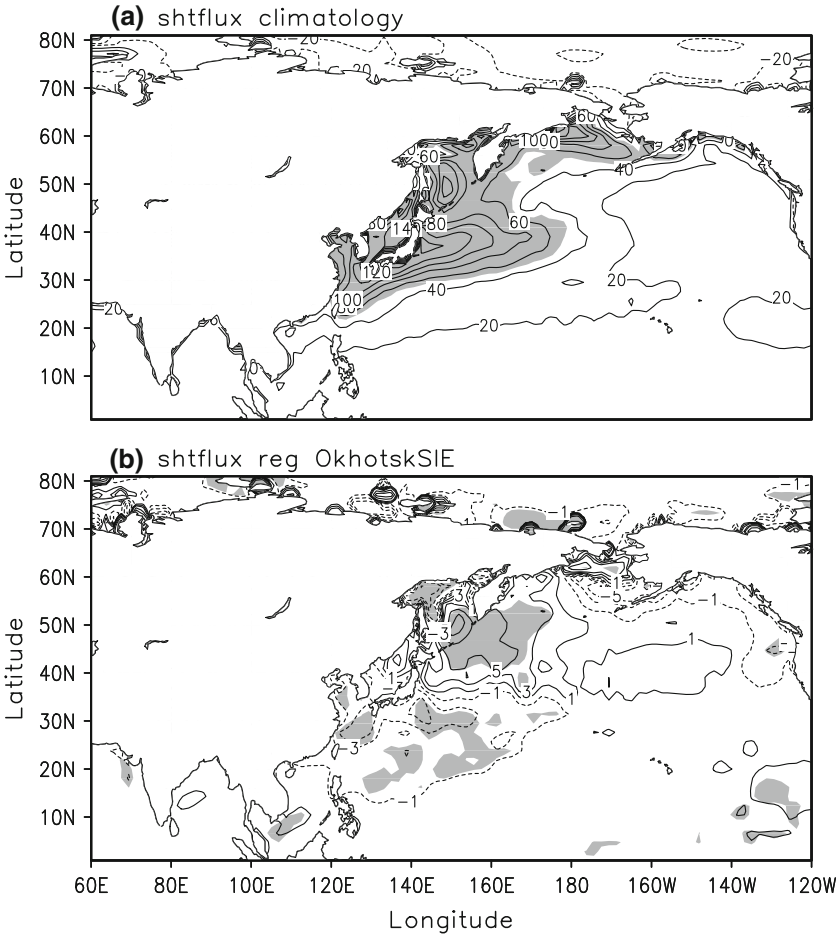

Fig. 4 **a** Winter net sensible heat flux climatology for the period of 1979–2008 (positive values are the heat flux from ocean to atmosphere; *shaded areas* denote that values exceed 50 W/m^2); **b** sensible heat flux anomalies corresponding to the OSI above +1 standard deviation, with the *shaded areas* denoting that the regression coefficients are significant at the 95% level (unit W/m^2)

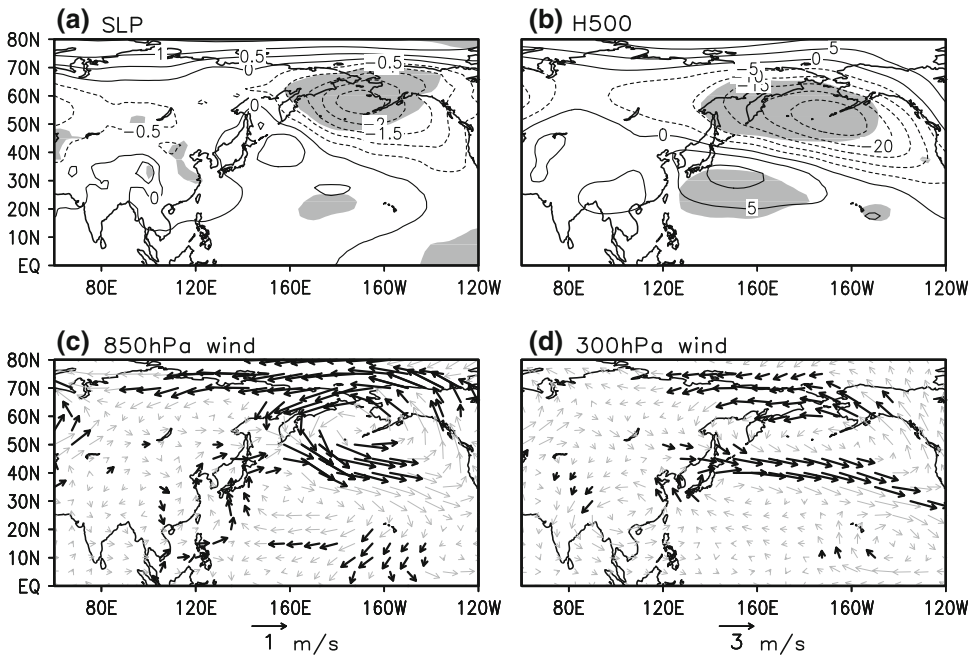

Fig. 5 Winter atmospheric circulation changes corresponding to the OSI above +1 standard deviation. **a** Sea level pressure (unit hPa); **b** 500 hPa geopotential height (unit gpm); **c** 850 hPa horizontal wind field (unit m/s); and **d** 300 hPa horizontal wind field (unit m/s). *Shaded areas* (in **a** and **b**) and *bold black vectors* (in **c** and **d**) denote that regression coefficients are above the 95% significance level

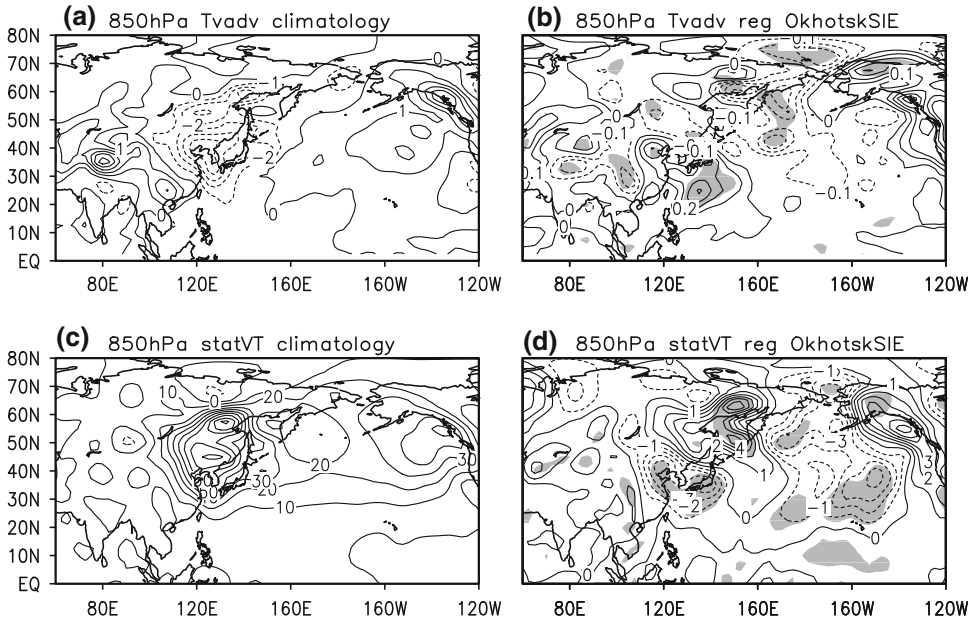

Fig. 6 **a** 850 hPa winter climatology of temperature advection by meridional winds; **b** 850 hPa meridional temperature advection anomalies corresponding to OSI above +1 standard deviation, with *shaded area* denoting the coefficients above the 95% significance level (unit °C/day). **c**, **d** Same as **a** and **b**, but for 850 hPa meridional heat flux due to stationary eddies (positive values are the poleward heat flux, unit °C m s^{-1})

$$\frac{\partial T}{\partial t} = \underbrace{-\vec{U}\cdot\nabla T}_{(1)} \underbrace{-\omega\left(\frac{\partial T}{\partial p} - \frac{RT}{C_p p}\right)}_{(2)} + \underbrace{Q_{te}}_{(3)} + \underbrace{Q_{se}}_{(4)} + \underbrace{Q}_{(5)}$$

where

$$Q_{te} = -\frac{\partial\left[\overline{u'T'}\right]}{\partial x} - \frac{\partial\left[\overline{v'T'}\right]}{\partial y}$$

$$Q_{se} = -\frac{\partial\left[\overline{u^*T^*}\right]}{\partial x} - \frac{\partial\left[\overline{v^*T^*}\right]}{\partial y}$$

T is the air temperature, $\vec{U}$ the horizontal velocity, ω the vertical velocity, C_p the specific heat of dry air at constant pressure, R the gas constant for dry air, p the pressure, Q_{te} and Q_{se} the heating rates due to eddy heat flux convergence of transient and stationary eddies, respectively (the overbars and parentheses refer to the monthly and zonal average, while the superscript primes ($'$) and stars refer to the deviation from the monthly and zonal average), and Q the diabatic heating.

The factors capable of influencing the temperature tendency are: (1) horizontal temperature advection, (2) temperature convection (adiabatic heating/cooling associated with the descent/ascent), (3) the heating rate due to heat flux convergence associated with stationary eddies, (4) the heating rate due to heat flux convergence associated with transient eddies, and (5) the diabatic heating (including the heating rates due to net sensible heat flux, latent heat release, and radiative processes). Because diabatic heating is difficult to quantify, we only estimate the changes in the first four terms on the right side of the equation in association with the OSI anomaly. The latitude–pressure sections of heating rate due to temperature advection and convection corresponding to the OSI above one standard deviation are shown in Fig. 7. Both the meridional temperature advection (Fig. 7b) and the convection (Fig. 7c) act to warm (cool) the lower (higher) latitudes, with the maximums at the middle and upper troposphere, while the zonal temperature advection tends to compensate this tropospheric heating in the WP region to some extent (Fig. 7a).

Figure 8 shows the heating rate due to the eddy heat flux convergence of transient and stationary eddies. The anomalous heat flux convergence (divergence) of stationary eddies has the potential to warm (cool) the lower (higher) latitudes (Fig. 8a). In contrast, the significant divergence anomalies (cooling) of transient eddy heat flux occur at the middle latitude band (about 40°N) (Fig. 8b).

This heat budget diagnosis indicates that the WP warming results from these three processes: (1) the warm advection by the anomalous southerly flow (weakening of EAWM), (2) the adiabatic heating by the descent flow, and (3) the stationary eddy heat flux convergence. The zonal heat advection leads to cooling of the middle and upper troposphere, somewhat compensating the heating effect by other factors. Figure 9 summarizes the total tropospheric heating and the contributions of various factors over the WP region (15–40°N mean). Total tropospheric temperature rises by about 0.25°C in accordance with the OSI above plus one standard deviation. At the lower troposphere (below 600 hPa), about 50% of the temperature increase comes from the contribution of temperature advection by meridional winds. The next is the adiabatic heating due to descent, which accounts for 30% of the temperature increase. The stationary eddy heat flux convergence contributes up to 15% of the total warming. It

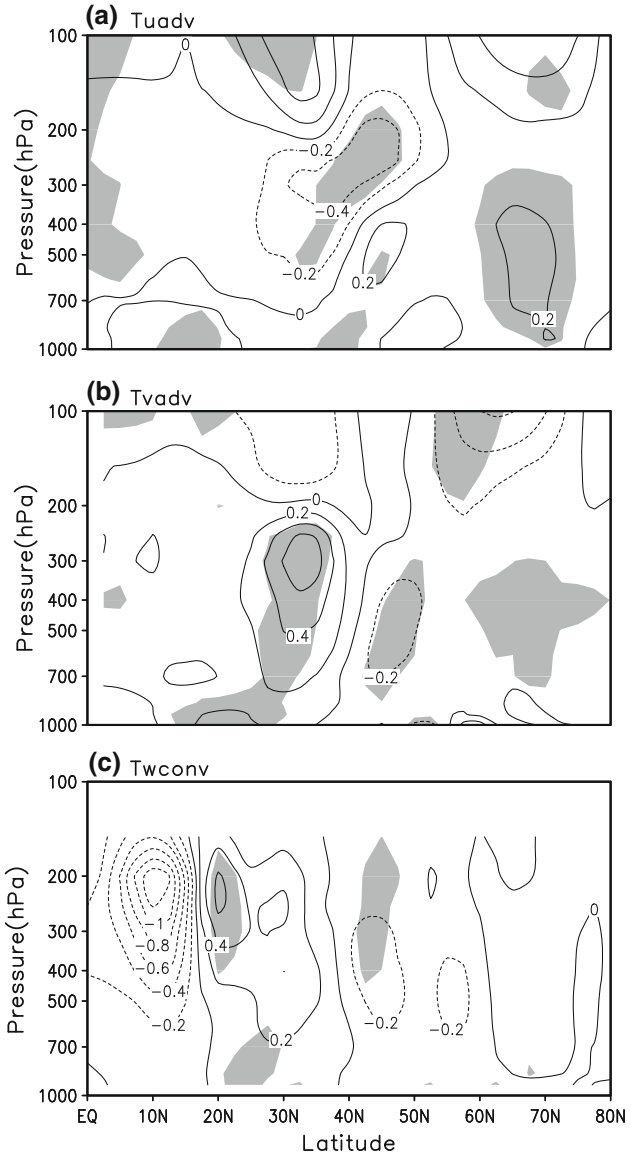

Fig. 7 **a** Latitude–pressure section of winter zonal temperature advection anomalies over Western Pacific region (120–160°E) corresponding to the OSI above +1 standard deviation, with the *shaded area* representing the regression coefficients above the 95% significance level (unit °C/day). Same as **a**, but for **b** meridional temperature advection and **c** the vertical temperature convection

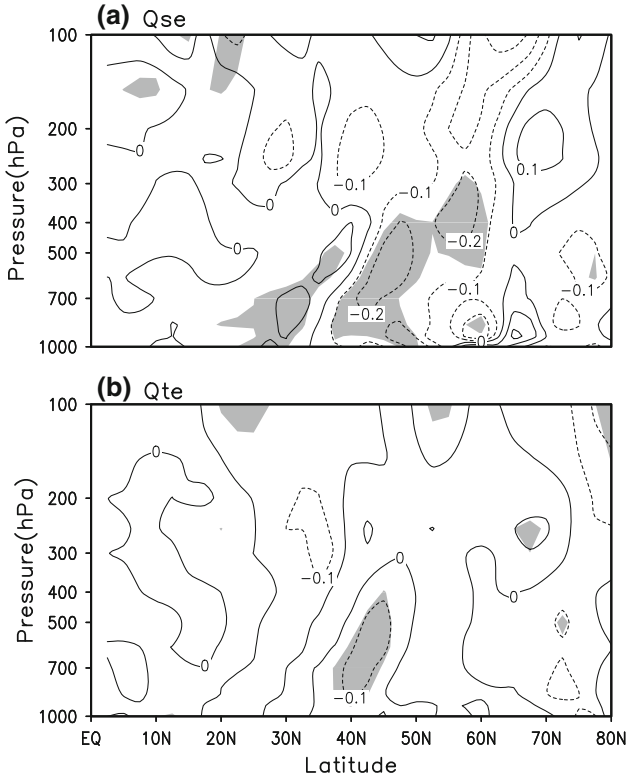

Fig. 8 Same as Fig. 7, but for **a** heating rate due to stationary eddy heat flux convergence; **b** heating rate due to transient eddy heat flux convergence

should be noted that the cooling due to zonal temperature advection compensates the warming due to meridional temperature advection to a large extent. Thus the horizontal temperature advection as a whole makes much less contribution than the other two factors. In this sense, the adiabatic heating and the stationary eddy heat flux convergence may be the most important factors that relate the subtropical temperature anomaly to the ice extent in the Sea of Okhotsk.

We also conducted the heat budget diagnosis for the subpolar region (42–60°N mean), covering the OS (Fig. 10). Along with the ice expansion in the OS, the tropospheric temperature in the subpolar region decreases about 0.4°C. Still the major contributors are meridional temperature advection, the adiabatic heating due to vertical movement, and the stationary eddy heat flux divergence. These three terms have comparable magnitudes in the middle and upper troposphere. But in the lower troposphere, the cooling due to stationary eddy heat flux divergence dominates the other two factors. The zonal temperature advection, in contrast, warms up the middle troposphere and cools down the upper troposphere. Note that the total cooling (−0.4°C) over the OS exceeds the warming (0.25°C) in the WP region. The net cooling can be mainly attributed to the excessive heat flux divergence due to stationary eddies over the OS, compared to the much smaller eddy heat flux convergence in the WP. This conclusion is consistent with Honda et al. (1999), who suggested that the anomalous OS ice may generate the stationary eddy activity change, leading to the remote response in the Bering Sea and Alaska.

6 Summary and discussion

Using the method of linear regression, we investigated the connection between the winter temperature over the WP

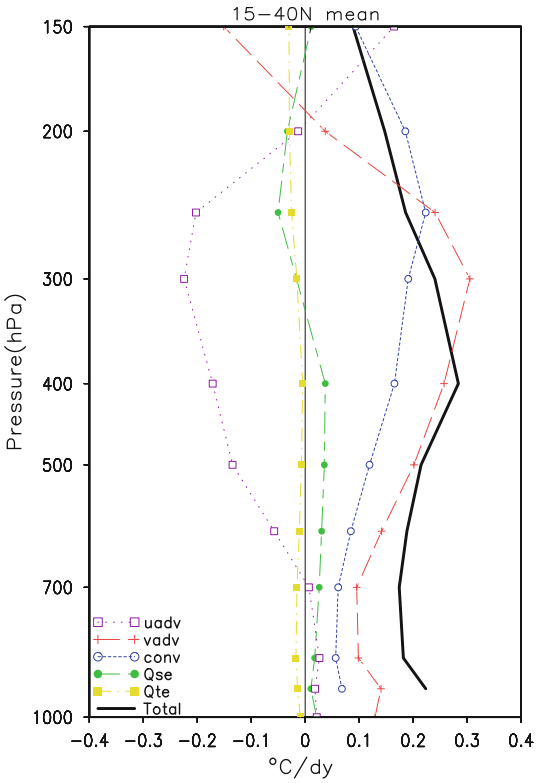

Fig. 9 Tropospheric subtropical Western Pacific (120–160°E, 15–40°N mean) heating rates due to various processes corresponding to the OSI above +1 standard deviation

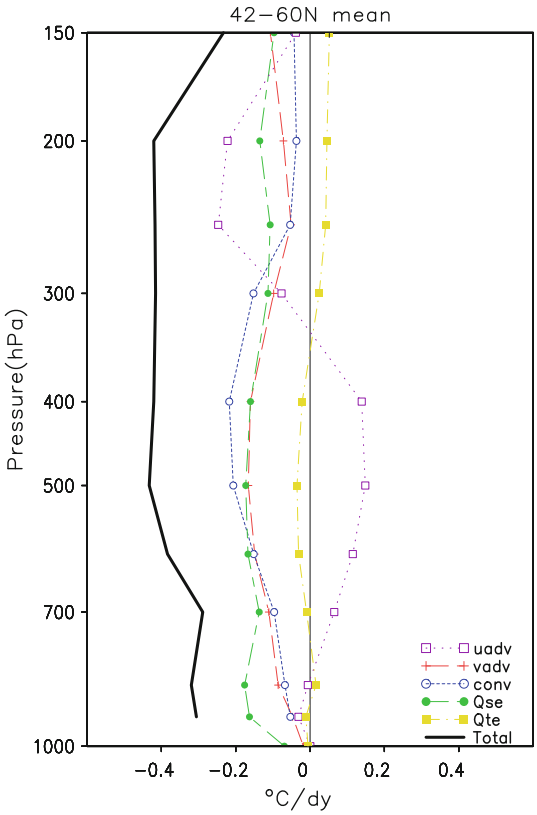

Fig. 10 Same as Fig. 9, but for subpolar region covering the Sea of Okhotsk (120–160°E, 42–60°N mean)

and the OS ice extent. The surface warming in the WP is accompanied by the cooling in the OS and adjacent areas associated with the OS ice expansion. The temperature dipole pattern extends from the surface up to the middle troposphere, which is driven dynamically by the anomalous meridional atmospheric circulation. The ice expansion in the OS is associated with the deepening of the Aleutian Low and the East Asian trough, and the enhanced EAWM poleward of 40°N. Along with the cyclonic anomaly in the high latitudes, an anomalous anticyclone appears equatorward of 40°N. The anomalous southerly advects the warm, moist air from the low latitudes to the WP, thus leading to a milder winter in this region. By a detailed heat budget diagnosis, we further reveal that when the OSI is above one standard deviation, the WP warms up by approximately 0.25°C throughout the whole troposphere. Nearly one half of the lower tropospheric warming is due to temperature advection by meridional winds. In addition, about 30 and 15% of the temperature increase at the lower troposphere level can be accounted for by the adiabatic heating due to the vertical movement and by the stationary eddy heat flux convergence, respectively. In the middle and upper troposphere, the strong heating owing to the meridional advection and vertical convection is partly cancelled by the zonal temperature advection, yielding the almost uniform warming throughout the troposphere. In the meanwhile, the adiabatic heating and the stationary eddy heat flux also coordinate to cool down the OS region, and the zonal and meridional temperature advection almost cancel each other, yielding nearly zero effect for the cooling over OS region.

However, the significant correlation between the Sea of Okhotsk ice extent and subtropical air temperature does not signify a cause and effect relation or the internal dynamics. We referred to Wang et al. (2010a), and compared our results (Fig. 3) with the same regression coefficient patterns using their EAWM index—the principal component of the second EOF modes for the winter mean 2-m air temperature in the EAWM domain (Fig. 11, left panel). Figure 11 (left panel) looks very close to Fig. 3 in our manuscript, though several small discrepancies can be distinguished. In light of the significant correlation between the EAWM index and our OSI (correlation coefficient is 0.46 for 30 winters), we constructed a new index by removing the effect of EAWM from the original OSI. The format is written as $\mathrm{OSI}_{(-\mathrm{EAWM})} = \mathrm{OSI} - \mathrm{EAWM} * R(\mathrm{EAWM}, \mathrm{OSI})$, where R(EAWM, OSI) denotes the regression coefficient of OSI on the EAWM index. After removing the effect of EAWM, the correlations between the SST/SAT over the subtropical WP and the

new OSI $_{(-\mathrm{EAWM})}$ index are largely decreased, though the correlations over the higher latitudes remain unchanged (Fig. 11a, b, right panel). Further analysis indicates that without the effect of EAWM, the dipole pattern of regression coefficients of tropospheric air temperature on the OSI almost disappears (Fig. 11c, right panel). All this evidence demonstrates that the connection between the Sea of Okhotsk ice extent and subtropical air temperature may largely be attributed to the large-scale atmospheric anomalies.

Nevertheless, the role of the Sea of Okhotsk ice in modulating the regional atmospheric circulation cannot be neglected. The sea ice may modulate the exchange of radiation, sensible heat flux, and momentum between the atmosphere and the ocean (Budikova 2009). Using the daily data, we investigated the lead–lag correlation between the Sea of Okhotsk ice extent and the surface sensible heat flux and 2-m air temperature over the Okhotsk region (140–155°E, 45–60°N average) as shown in Fig. 12. The winter (December–February) Sea of Okhotsk ice extent anomalies are positively correlated with the preceding surface heat flux and negatively correlated with the following surface heat flux (Fig. 12a). In contrast, the correlations between the air temperature and sea ice cover are always negative regardless of the leading or lagging (Fig. 12b). This manifests the thermal effect of sea ice on the atmosphere—the cold winter (low temperature) is always associated with the increase of heat flux from ocean to atmosphere, thus preconditions for the ice cover growth. The ice cover, in turn, insulates the exchange of heat between ocean and atmosphere, resulting in the less sensible heat flux and lower temperature in the later period. This thermal feedback mechanism may lead to the intensification of the meridional temperature gradient, and then the acceleration of the mid-latitude jet stream. In this way,

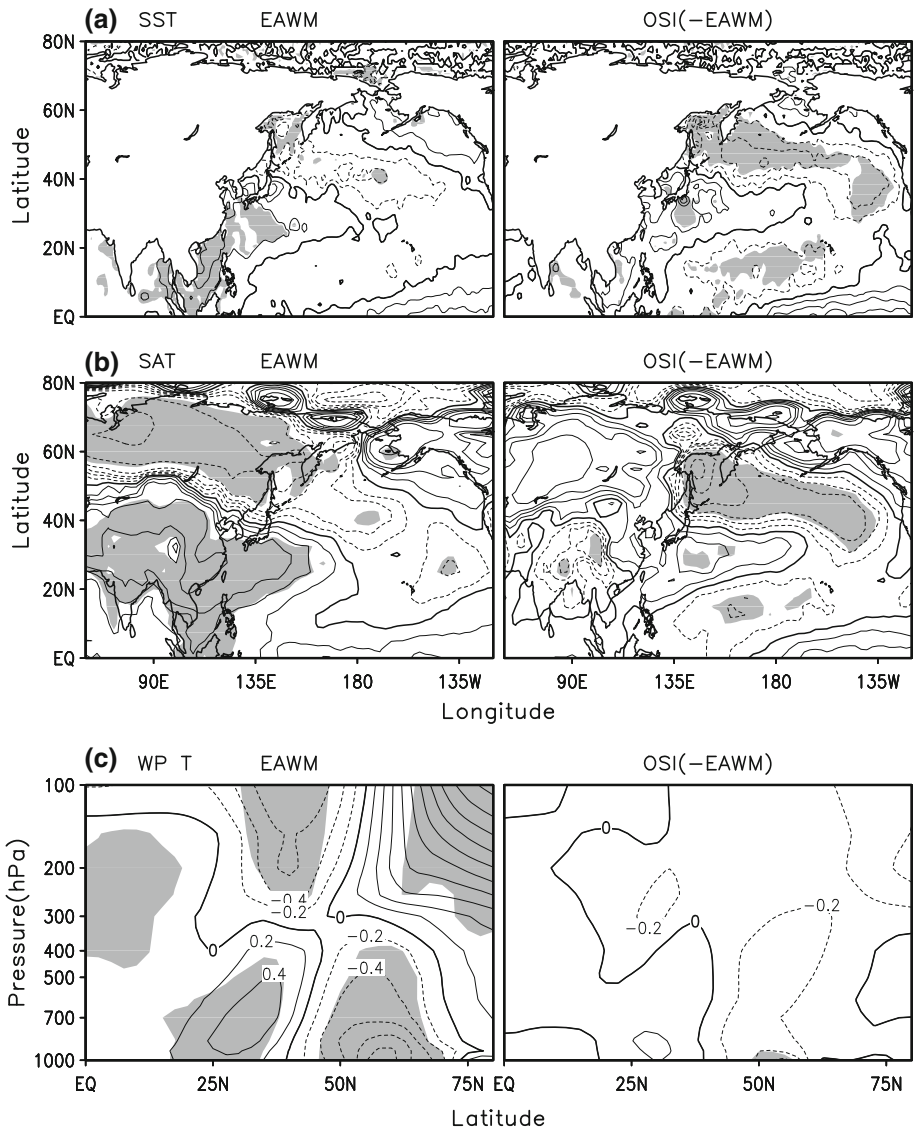

Fig. 11 Same as Fig. 3, but the regressed on the EAWM index (Wang et al. 2010a, *left panel*) and on the new OSI after removing the effect of EAWM (*right panel*; for details see text)

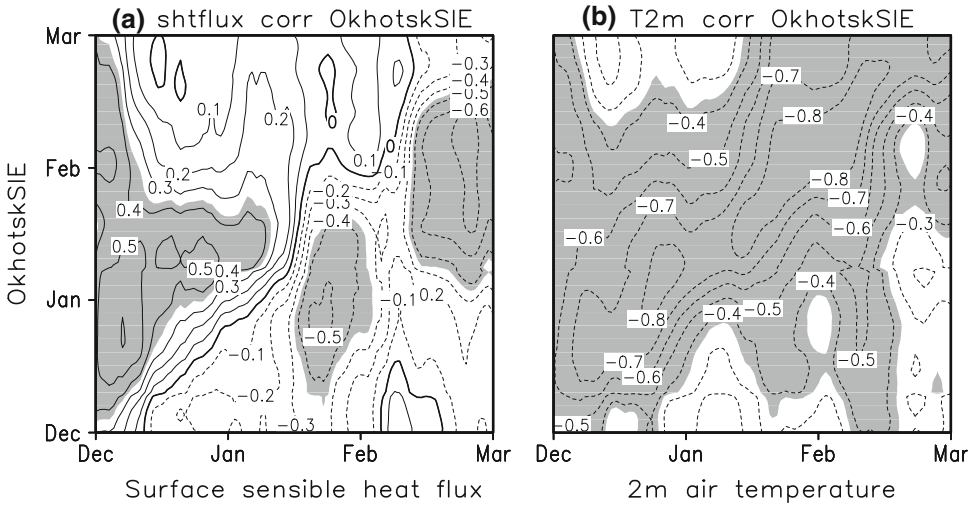

Fig. 12 Lead–lag correlation between daily Sea of Okhotsk ice extent and net sensible heat flux (**a**) and 2-m air temperature (**b**) during winter (December–February) period. *Shaded areas* denote that the correlation coefficients are above the 95% significance level

the Sea of Okhotsk ice may feed back to the local atmospheric circulation.

Acknowledgments We thank three reviewers for their insightful suggestions and comments. This study is supported by the NSFC under contract of 41006113 and 40821063, by the National Basic Research Program of China (2007CB411803), and by MELRS0920 of Xiamen University (for Yang and Hu). Wang is supported by the RUSALCA modeling project of NOAA Office of Arctic Research.

References

Ambaum MHP, Hoskins BJ, Stephenson DB (2001) Arctic Oscillation or North Atlantic Oscillation? J Clim 14:3495–3507

Armstrong AE, Tremblay LB, Mysak LA (2003) A data-model intercomparison study of Arctic sea-ice variability. Clim Dyn 20:465–476

Budikova D (2009) Role of Arctic sea ice in global atmospheric circulation: a review. Glob Planet Change 68:149–163

Chiang JCH, Bitz CM (2005) Influence of high latitude ice cover on the marine Intertropical Convergence Zone. Clim Dyn 25:477–496

Clark MP, Serreze MC (2000) Effects of variations in East Asian snow cover on modulating atmospheric circulation over the North Pacific Ocean. J Clim 13:3700–3710

Fang Z, Wallace JM (1994) Arctic sea ice variability on a timescale of weeks and its relation to atmospheric forcing. J Clim 7:1897–1914

Gong D-Y, Ho C-H (2002) The Siberian High and climate change over middle to high latitude Asia. Theor Appl Climatol 72:1–9

Gong D-Y, Wang S-W, Zhu J-H (2001) East Asian winter monsoon and Arctic oscillation. Geophys Res Lett 28(10):2073–2076

Honda M, Yamazaki K, Nakamura H, Takeuchi K (1999) Dynamic and thermodynamic characteristics of atmospheric response to anomalous sea-ice extent in the Sea of Okhotsk. J Clim 12:3347–3358

Kalney E et al (1996) The NCEP/NCAR 40-year reanalysis project. Bull Am Meteor Soc 77:437–471

Lau N-C, Nath MJ (2000) Impact of ENSO on the variability of the Asian–Australian Monsoons as simulated in GCM experiments. J Clim 13:4287–4309

Liu J, Zhang Z, Horton RM, Wang C, Ren X (2007) Variability of North Pacific sea ice and East Asia–North Pacific winter climate. J Clim 20:1991–2001

Parkinson CL (1990) The impact of the Siberian high and Aleutian low on the sea-ice cover of the Sea of Okhotsk. Ann Glaciol 14:226–229

Parkinson CL, Rind D, Healy RJ, Martinson DG (2001) The impact of sea ice concentration accuracies on climate model simulations with the GISS GCM. J Clim 14:2606–2623

Raymo ME, Rind D, Ruddiman WF (1990) Climatic effects of reduced Arctic sea ice limits in the GISS II general circulation model. Paleoceanography 5:367–382

Rayner NA, Parker DE, Horton EB, Folland CK, Alexander LV, Rowell DP, Kent EC, Kaplan A (2003) Global analyses of sea surface temperature, sea ice, and night marine air temperature since the late nineteenth century. J Geophys Res 108(D14):4407. doi:10.1029/2002JD002670

Rodionov SN, Overland JE, Bond NA (2005) The Aleutian Low and winter climatic conditions in the Bering Sea. Part I: classification. J Clim 18:160–177

Royer JF, Planton S, Deque M (1990) A sensitivity experiment for the removal of Arctic sea ice with the French spectral general circulation model. Clim Dyn 5:1–17

Sasaki YN, Katagiri Y, Minobe S, Rigor IG (2007) Autumn atmospheric preconditioning for interannual variability of wintertime sea-ice in the Okhotsk Sea. J Oceanogr 63:255–265

Walsh JE (1995) A sea ice database. In: Folland C, Rowell D (eds) Workshop on simulations of the climate of the twentieth century using GISST, 28–30 November 1994. Hadley Centre for Climate Prediction and Research CRTN 56, pp 54–58

Wang J, Ikeda M (2000) Arctic oscillation and Arctic sea-ice oscillation. Geophys Res Lett 27(9):1287–1290

Wang C, Weisberg RH, Virmani JI (1999) Western Pacific interannual variability associated with the El Niño–Southern Oscillation. J Geophys Res 104:5131–5149

Wang B, Wu R, Fu X (2000) Pacific-East Asian teleconnection: how does ENSO affect East Asian climate? J Clim 13:1517–1536

Wang J, Jin M, Musgrave D, Ikeda M (2004) A numerical hydrological digital elevation model for freshwater discharge into the Gulf of Alaska. J Geophys Res 109:C07009. doi:10.1029/2002JC001430

Wang B, Wu Z, Chang C-P, Liu J, Li J, Zhou T (2010a) Another look at interannual-to-interdecadal variations of the East Asian

Winter Monsoon: the northern and southern temperature modes. J Clim 23:1495–1512
Wang J, Bai X, Wang D-X, Hu H, Yang X-Y (2010b) Interannual variability of the East Asia winter monsoon, as controlled by the Siberian High and Arctic Oscillation: driving downwelling in the western Bering Sea. Submitted to Aquat Ecosyst Health Manag
Wu B, Wang J (2002) Winter Arctic Oscillation, Siberian High and the East Asia winter monsoon. Geophys Res Lett 29(19):1897–1900